Experimental test of the Collins-Gisin-Linden-Massar-Popescu inequality for multisetting and multidimensional orbital angular momentum systems

Dongkai Zhang,[1,2,*] Xiaodong Qiu,[2] and Lixiang Chen[2,†]

[1]*College of Information Science and Engineering, Fujian Provincial Key Laboratory of Light Propagation and Transformation,
Huaqiao University, Xiamen 361021, China*
[2]*Department of Physics, Xiamen University, Xiamen 361005, China*

Characterizing high-dimensional entangled states holds pivotal significance in quantum information science and technology. Recent theoretical progress has been made to extend the Collins-Gisin-Linden-Massar-Popescu (CGLMP) inequality into a general scenario with multisetting and multidimensional systems. Here, by employing two-photon orbital angular momentum entanglement, we conduct an experiment to demonstrate the CGLMP inequality across multiple settings and outcomes. Our experimental results violate the CGLMP inequality by more than 12 standard deviations, demonstrating that the maximum violation increases with both dimension and setting. Furthermore, we reveal, both theoretically and experimentally, the logical connection between the CGLMP inequality and the general Hardy's paradox. Intriguingly, our analysis establishes that, even in high-dimensional systems, Hardy's paradox can be regarded as a special instance of Bell inequality, with their respective bounds aligning under the no-signaling principle and the information causality principle. Our work may advance the foundational understanding of quantum correlations in high-dimensional quantum systems.

I. INTRODUCTION

In 1935 Einstein, Podolsky, and Rosen (EPR) formulated a renowned argument questioning the completeness of quantum mechanics [1]. In 1964 Bell refuted the EPR argument against quantum mechanics and showed that certain correlations arising from the measurements of a quantum system by distant observers cannot be accounted for within a classical, deterministic local model grounded in "elements of reality" [2]. Following Bell's contributions, various versions of Bell inequalities were developed, expanding our understanding of nonlocality [3–8]. In 2002, Collins and co-workers extended Bell inequality to high-dimensional systems, namely Collins-Gisin-Linden-Massar-Popescu (CGLMP) inequality [4]. Subsequently, Dada and co-workers established an experimental verification of CGLMP inequality, observing violations of Bell-type inequalities up to 12-dimensional systems [5]. In 2008, Zohren and co-workers proposed a novel version of the CGLMP inequality, effectively simplifying the intricate logic of the original CGLMP inequality and revealing that the optimal state is far from maximally entangled [6]. Recent progress was also made to generalize this simplified version of CGLMP inequality to multisetting scenarios [7], while the CGLMP inequality for multisetting and multidimensional systems has not yet been conducted in experimental implementations.

Exploring the experimental test of the CGLMP inequality for a broader (k, d) scenario, i.e., k-setting d-dimensional

system, involves significant theoretical and experimental advancements. From a theoretical perspective, it deepens our understanding of nonlocal quantum correlations [9,10], sharpens the contradiction between quantum mechanics and classical theory [6,7], and significantly reduces the critical detection efficiency needed for more robust tests of quantum nonlocality [11–13]. From an application standpoint, the significance of the general (k, d) version of the CGLMP inequality becomes pronounced in circumstances where the conventional Bell inequality falls short. First, quantum key distribution (QKD) protocols based on high-dimensional quantum states offer advantages in terms of security and information capacity [14,15]. Exploring the CGLMP inequality in QKD protocols can develop new tests and criteria for assessing the security of high-dimensional QKD protocols, enabling the implementation of more robust and efficient quantum cryptographic systems [16,17]. Moreover, the Bell inequality with a large k can further improve the security of QKD protocols [18]. Second, quantum computation using high-dimensional states can reduce circuit complexity and offer significant advantages in various applications within the noisy intermediate-scale quantum (NISQ) era [19–21]. Recent advancement introduced a protocol for black-box equivalence checking of quantum circuits, leveraging the CGLMP inequality as a pivotal quantum property [22]. Third, high-dimensional quantum states are valuable in quantum metrology, as they enable enhanced precision and sensitivity in measurements [23,24]. The CGLMP inequality plays a key step in this context, serving as a tool for examining and validating the quantum properties of high-dimensional states [25]. In this article, we leverage high-dimensional orbital angular momentum (OAM) entanglement in two-photon systems to

---

*Contact author: zhangdk@hqu.edu.cn

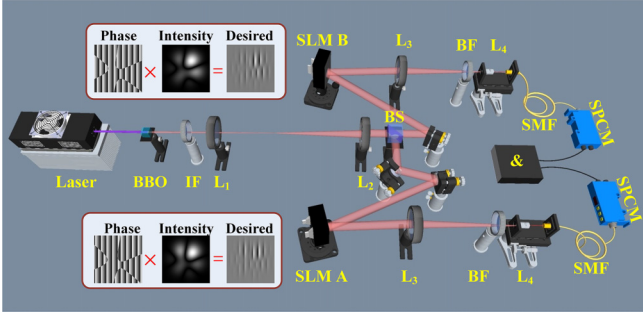†Contact author: chenlx@xmu.edu.cn

012202-1

FIG. 1. Experimental setup for demonstrating the CGLMP inequality with high-dimensional OAM entanglement. Top and bottom insets are examples of intensity and phase of measurement modes and the desired holograms displayed in SLM.

experimentally demonstrate the violation of the simplified version of CGLMP inequality across scenarios with multiple settings and outcomes. Our experimental observations reveal a significant increase in the violation of the CGLMP inequality as the dimension d and setting k increase, highlighting a sharper contradiction between quantum mechanics and classical theory. Additionally, we juxtapose our theoretical and experimental findings with those derived from the Clauser-Horne inequality of the general Hardy's paradox [26], thereby establishing a logical connection between them. Specifically, our analysis emphasizes that, within the high-dimensional systems, Hardy's paradox can be regarded as a specific instance of Bell inequalities. This connection ensures that the boundaries of these two nonlocal theories remain consistent under the no-signaling principle and the information causality principle.

II. EXPERIMENTAL SETUP AND RESULTS

In contrast to the spin angular momentum of light, the orbital angular momentum (OAM) of light possesses an intrinsic capability for high-dimensional quantum information processing [27–29]. Here, we adopt high-dimensional OAM entanglement states to prove the simplified version of CGLMP inequality within scenarios involving multiple settings and outcomes. Our experimental configuration is illustrated in Fig. 1. We generate OAM entangled photons by pumping a β-barium borate (BBO) crystal under frequency-degenerate type-I spontaneous parametric down-conversion (SPDC). Lenses (f1 = 100 mm and f2 = 400 mm) form a 4f system and image the plane of the BBO on the spatial light modulator (SLM). Each SLM is loaded with specially designed holographic gratings for the precise preparation of the optimal measurement OAM states [as defined in Eq. (4) and Eq. (5)] and for carrying out entanglement concentration. After interacting with the SLMs, photons are coupled into a single-mode fiber (SMF) using collecting lenses (f3 = 1000 mm and f4 = 2 mm) and detected by single photon detectors. Both single photon detectors are connected to a coincidence circuit for acquiring the coincidence counts.

In recent years, there has been a burgeoning interest in characterizing high-dimensional entangled states [30], driven by the recognition of their significance in quantum information science. One elegant and logically straightforward

method is through Bell inequality with k settings and d outcomes, such as the simplified version of CGLMP inequality, expressed as [6,7]

$$P(A^k \geqslant B^k) + \sum_{i=2}^{k} P(A^i < B^{i-1})$$

$$+ \sum_{i=2}^{k} P(B^{i-1} < A^{i-1}) + P(A^1 < B^k) \geqslant 1, \qquad (1)$$

where $P(A^i < B^j) = \sum_{s<t} P(A^i_s, B^j_t)$ represents the joint conditional probability that the result of A^i is strictly smaller than the result of B^j. Here, $i, j \in \{1, 2, \ldots, k\}$ and $s, t \in \{0, 1, \ldots, d-1\}$, and thus $P(A^i_s, B^j_t)$ is the probability that, when Alice and Bob measure in settings i and j, respectively, Alice's measurement returns outcome s and Bob's measurement returns outcome t. It is noteworthy that extending Bell inequality to high-dimensional multisetting scenarios not only contributes to more efficient and robust quantum communication tasks [30] but also brings measurement results closer to the no-signaling bound [7]. Here, we propose a simple transformation of the CGLMP inequality, making it equivalent in form to the Clauser-Horne inequality of the general Hardy's paradox. This transformation enables us to conduct theoretical and experimental comparison between Bell inequality and Hardy's paradox in a broader (k, d) scenario and thus guide us to a deeper understanding of quantum nonlocality. For a given (k, d) scenario, by substituting $P(A^k \geqslant B^k) = 1 - P(A^k < B^k)$ into Eq. (1), we can construct a simplified version of the CGLMP inequality (also the Clauser-Horne inequality of the general Hardy's paradox; see more details in the Discussion section)

$$S_{(k,d)} = P(A^k < B^k) - \sum_{i=2}^{k} P(A^i < B^{i-1})$$

$$- \sum_{i=2}^{k} P(B^{i-1} < A^{i-1}) - P(A^1 < B^k) \leqslant 0. \quad (2)$$

The proof of the inequality (2) is straightforward, starting with the evident statement $\cap_{i=2}^{k}(\{A^i \geqslant B^{i-1}\} \cap \{B^{i-1} \geqslant A^{i-1}\}) \cap \{A^1 \geqslant B^k\} \subseteq \{A^k \geqslant B^k\}$ [6,7], where $\{A^i \geqslant B^j\}$ represents the mathematical set of the outcomes of A^i greater than or equal to the outcomes of B^j. Taking the complement of both sides, it holds that

$$\{A^k < B^k\} \subseteq \cup_{i=2}^{k}(\{A^i < B^{i-1}\} \cup \{B^{i-1} < A^{i-1}\}) \cup \{A^1 < B^k\}.$$
$$(3)$$

It is worth noting that, within a given Bell scenario, classical probability distributions manifest as convex combinations of entirely deterministic probability distributions, wherein probabilities are trivial, being either zero or one. Consequently, randomness is construed not as an inherent attribute but rather as a statistical phenomenon within classical probability frameworks. Thus it logically follows that $P(A^k < B^k) \leqslant \sum_{i=2}^{k} P(A^i < B^{i-1}) + \sum_{i=2}^{k} P(B^{i-1} < A^{i-1}) + P(A^1 < B^k)$, thereby completing the proof.

Here, by exploring two-photon OAM entanglement generated via SPDC, we can translate the inequality (2)

into an experimental implementation. In SPDC, the high-dimensional OAM entangled state is represented as $|\Psi\rangle_{AB} = \sum_\ell c_\ell |\ell\rangle_A |-\ell\rangle_B$, where c_ℓ denotes the probability amplitude of detecting one signal photon (A) with $\ell\hbar$ OAM and its corresponding idler photon (B) with $-\ell\hbar$ OAM [31]. In our pursuit to investigate a larger yet finite subspace for formulating the CGLMP inequality with OAM, we consider the optimal Bell states, $|\psi_d\rangle = \sum_{m=0}^{d-1} \lambda_m |\ell_m\rangle_A |-\ell_m\rangle_B$, within a designated d-dimensional OAM subspace, where λ_m represents real numbers satisfying the normalization condition $\sum_{m=0}^{d-1} \lambda_m^2 = 1$. In this scenario, Alice and Bob can each perform k sets of measurement, on which the measurement outcomes range from 1 to d. Their von Neumann measurements are defined as $|A_s^i\rangle\langle A_s^i|$ and $|B_t^j\rangle\langle B_t^j|$, respectively. The optimal measurements can be derived by performing extensive numerical analysis using semidefinite programs [7] as

$$|A_s^i\rangle = \frac{1}{\sqrt{d}} \sum_{m=0}^{d-1} \exp\left[I\frac{2\pi}{d}m(s+\alpha_i)\right]|\ell_m\rangle_A, \qquad (4)$$

$$|B_t^j\rangle = \frac{1}{\sqrt{d}} \sum_{m=0}^{d-1} \exp\left[I\frac{2\pi}{d}m(-t-\beta_j)\right]|-\ell_m\rangle_B, \qquad (5)$$

where s and t represent the outcomes of Alice's and Bob's measurements, respectively, and $I = \sqrt{-1}$ is an imaginary number. Then, the probability $P(A^i < B^j)$ in a specific d-dimensional OAM subspace can be expressed as

$$P(A^i < B^j) = \sum_{s=0}^{d-2} \sum_{t=s+1}^{d-1} \left|\langle A_s^i|\langle B_t^j|\psi_d\rangle\right|^2. \qquad (6)$$

Here we choose $\alpha_i = i/k - 1/2k$ for $i = 1, 2, \ldots, k$, $\beta_j = j/k$ for $j = 1, 2, \ldots, k-1$, and $\beta_k = 0$; then, from the derivation procedure in Ref. [7], we obtain the Bell expression $S_{(k,d)}$ as

$$S_{(k,d)} = 1 - \sum_{m,n=0}^{d-1} M_{mn}\lambda_m\lambda_n. \qquad (7)$$

Here, M is the $d \times d$ matrix defined by $M_{mm} = k - (k-1)/d$ and $M_{mn} = -k \sin[\eta(k-1)/k]/[d \sin(\eta)]$, for $m \neq n$, where $\eta = \pi(m-n)/d$. Thus the problem of finding the maximal quantum violation of the inequality (2) reduces to finding the smallest eigenvalue of M and the entangled state responsible for this violation is the corresponding eigenvector of M. After some algebra, we derive the optimal entangled states that yield the maximum value of S, as elaborated in Appendix A.

Our experimental design encompasses a broad multisetting and multidimensional scenario, denoted as (k, d), where we consider various combinations such as $k = 2, 3, 4, 5$, and $d = 2, 3, 4, 5, 6$ within the OAM subspaces. Through theoretical calculations, we find that, for a given dimension d, if the chosen approximate state resembles any of the four optimal states corresponding to $k = 2, 3, 4$, and 5, then, in these four cases, the theoretical values of Bell expression achieved by the approximate state closely approach the maximum achievable values by optimal states. Therefore, for each d-dimensional OAM subspace, we experimentally prepare an approximate state $|\psi_d^{\mathrm{app}}\rangle$. Subsequently, if its theoretical values of Bell expression in the $k = 2, 3, 4$, and 5 scenarios closely approach the maximum achievable values (see Appendix A for more details), we proceed with utilizing this state for measurements. These approximate states are denoted as

$$|\psi_2^{\mathrm{app}}\rangle_{AB} = 0.7071|+1\rangle_A|-1\rangle_B + 0.7071|-1\rangle_A|+1\rangle_B, \qquad (8a)$$

$$|\psi_3^{\mathrm{app}}\rangle_{AB} = 0.5960|+1\rangle_A|-1\rangle_B + 0.5288|+2\rangle_A|-2\rangle_B + 0.6042|-1\rangle_A|+1\rangle_B, \qquad (8b)$$

$$|\psi_4^{\mathrm{app}}\rangle_{AB} = 0.5392|+1\rangle_A|-1\rangle_B + 0.4613|+2\rangle_A|-2\rangle_B + 0.4521|-2\rangle_A|+2\rangle_B + 0.5404|-1\rangle_A|+1\rangle_B, \qquad (8c)$$

$$|\psi_5^{\mathrm{app}}\rangle_{AB} = 0.5030|+1\rangle_A|-1\rangle_B + 0.4200|+2\rangle_A|-2\rangle_B + 0.3671|+3\rangle_A|-3\rangle_B + 0.4301|-2\rangle_A|+2\rangle_B + 0.5009|-1\rangle_A|+1\rangle_B, \qquad (8d)$$

$$|\psi_6^{\mathrm{app}}\rangle_{AB} = 0.4700|+1\rangle_A|-1\rangle_B + 0.4011|+2\rangle_A|-2\rangle_B + 0.3493|+3\rangle_A|-3\rangle_B + 0.3530|-3\rangle_A|+3\rangle_B$$
$$+ 0.3880|-2\rangle_A|+2\rangle_B + 0.4701|-1\rangle_A|+1\rangle_B. \qquad (8e)$$

An additional challenge arises from the fact that the original OAM entangled states generated via SPDC deviate from these approximate states. To address this experimental issue, we employ entanglement concentration [5,26] to adapt the original state into the desired approximate state. In this procedure, we utilize local operations to adjust the weight amplitudes of each OAM mode by modifying the diffraction efficiencies of the blazed phase gratings. This way, we ensure a precise compensation of the weight amplitudes for OAM modes between the desired approximate states and the experimental states. Next, by substituting the OAM bases presented in Eq. (8) into Eq. (4) and Eq. (5), we can obtain the optimal measurements. For example for $|\psi_3^{\mathrm{app}}\rangle$, the optimal measurements can be reformulated with the OAM basis presented in Eq. (8b) as

$|A_s^i\rangle = \frac{1}{\sqrt{3}}(|+1\rangle_A + \omega_3^{s+\alpha_i}|+2\rangle_A + \omega_3^{2(s+\alpha_i)}|-1\rangle_A)$ and $|B_t^j\rangle = \frac{1}{\sqrt{3}}(|-1\rangle_B + \omega_3^{-t-\beta_j}|-2\rangle_B + \omega_3^{2(-t-\beta_j)}|+1\rangle_B)$, where $\omega_3 = \exp(I2\pi/3)$. By loading these OAM superposition states on the SLMs and recording the coincidence counts accordingly, we obtain the approximate Bell expressions, as shown in Fig. 2. Notably, all of these results violate the inequality (2) by more than 12 standard deviations. In Appendix B, we present a detailed exposition of measurement results that demonstrate a favorable agreement with quantum-mechanical predictions, thereby confirming the substantial enhancement of the maximum violation of the CGLMP inequality with increased dimension d and setting k. However, it is important to acknowledge that, due to inherent imperfections in state preparation and measurement, the experimental values of the
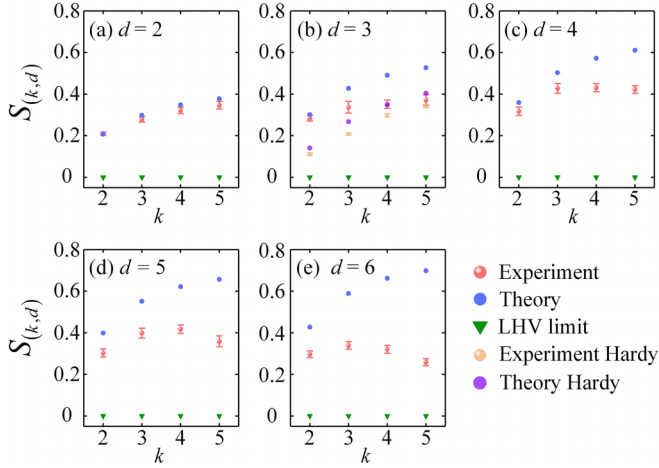
FIG. 2. Bell expression $S_{(k,d)}$ in (k,d) scenario: (a) $|\psi_2^{\mathrm{app}}\rangle$, (b) $|\psi_3^{\mathrm{app}}\rangle$, (c) $|\psi_4^{\mathrm{app}}\rangle$, (d) $|\psi_5^{\mathrm{app}}\rangle$, and (e) $|\psi_6^{\mathrm{app}}\rangle$. The red plot represents the experimental Bell expression, while the blue plot depicts the theoretically predicted violations based on approximate entangled states. Additionally, the green triangle represents the LHV (local hidden variables) limit in comparison with the experimental results. The purple plot represents the theoretical predictions for the Clauser-Horne inequality of the general Hardy's paradox and the orange plot bars showcase the corresponding experimental results.

Bell expression in Fig. 2 tend to be lower than the theoretical values.

III. DISCUSSION

Since Bell proposed the Bell inequality [2], various nonlocal theorems have emerged, including Hardy's paradox [26], Cabello's theorem [32], "all-versus-nothing" proof [33,34], and GHZ theorem [35]. Each of these theorems represents an independent logical framework to demonstrate nonlocality. An intriguing question arises: are these theories interconnected and is there a standardized mathematical framework that can unify them? This, in itself, poses an intriguing question and promises to uncover deeper physical insights. To address part of this question, specifically unifying Bell inequality and Hardy's paradox in the general (k,d) scenario, we conduct a thorough theoretical and experimental comparison between the CGLMP inequality and the general Hardy's paradox for general (k,d) systems. It is notable that while Bell inequalities and Hardy's paradox may initially seem conceptually disparate, with Bell inequalities primarily concerned with the statistical expectations of measurements and Hardy's paradox exploring the logical ramifications of possible and impossible events, recent theoretical developments within the (2, 2) scenario have revealed Hardy's paradox as a specialized subset of Bell inequalities [36]. Here, we focus on the connection between them in the general (k,d) scenario. Note that the inequality (2) is equivalent to the Clauser-Horne inequality of the general Hardy's paradox [26]. In essence, the general Hardy's paradox is equivalent to the CGLMP inequality with the exception that the Hardy scenario must obey $2k-1$ additional constraints on the measurements performed. More specifically, by introducing the constraints $\{A^i < B^{i-1}\} = \emptyset$, for $i = 2, 3, \ldots, k$,

$\{B^{i-1} < A^{i-1}\} = \emptyset$, for $i = 2, 3, \ldots, k$, and $\{A^1 < B^k\} = \emptyset$, into Eq. (3), we can straightforwardly obtain an empty set $\{A^k < B^k\} = \emptyset$. This implies that if $P(A^i < B^{i-1}) = 0$, for $i = 2, 3, \ldots, k$, $P(B^{i-1} < A^{i-1}) = 0$, for $i = 2, 3, \ldots, k$, and $P(A^1 < B^k) = 0$ hold, we can straightforwardly obtain an exactly zero probability $P(A^k < B^k) = 0$, which is the main deduction of the general Hardy's paradox [26,37]. Thus we assert that, within any (k,d) scenario, the general Hardy's paradox can be regarded as a special instance of the CGLMP inequality, offering a pathway to demonstrating nonlocality without invoking inequalities. Consequently, the maximal violation of the CGLMP inequality imposes an upper limit on the maximal fraction for the general Hardy's paradox, thereby exhibiting greater robustness against noise generated by deleterious environmental effects [38].

To analyze the quantum properties of the connections, we typically exploit maximally entangled states, denoted as $|\psi_d^{\mathrm{max}}\rangle = \frac{1}{\sqrt{d}} \sum_{m=0}^{d-1} |\ell_m\rangle_A |-\ell_m\rangle_B$, to compute the upper bound of the Bell expression. After some algebra in Appendix C, we calculated the Bell expression S for $|\psi_d^{\mathrm{max}}\rangle$ as

$$S_{(k,d)}^{\psi^{\mathrm{max}}} = \frac{1}{d^3} \sum_{m=1}^{d-1} \frac{(d-m)\sin^2\left(\frac{\pi}{2k}\right)}{\sin^2\left[\pi\left(-m+1-\frac{1}{2k}\right)/d\right]}$$
$$- \frac{(2k-1)}{d^3} \sum_{m=1}^{d-1} \frac{(d-m)\sin^2\left(\frac{\pi}{2k}\right)}{\sin^2\left[\pi\left(-m+\frac{1}{2k}\right)/d\right]}. \quad (9)$$

In the limit of large k, owing to $\lim_{k\to\infty} \sin^2(\pi/2k) = 0$, all other probabilities tend to zero, except for the first terms with $m = 1$, i.e., the first terms $P(A_s^k < B_t^k)$ in Eq. (2) with $t = s + 1$. This indicates that the inequality (2) approaches the general Hardy's paradox in the limit of large k, with the Bell expression (or maximal successful probability) being bounded by

$$S_{(\infty,d)}^{\psi^{\mathrm{max}}} = \lim_{k\to\infty} \frac{1}{d^3} \frac{(d-1)\sin^2(\pi/2k)}{\sin^2(-\pi/2kd)} = \frac{d-1}{d}. \quad (10)$$

Notably, we find the value is also the no-signaling bound for both the CGLMP inequality [7] and Hardy's paradox [39], suggesting that, in scenarios with numerous measurement settings, quantum theory converges towards the no-signaling bound. This theoretical finding provides compelling evidence that, even in high-dimensional systems, the no-signaling bounds for CGLMP inequality and the general Hardy's paradox coincide. In the limit of large k and d, the maximal successful probability can reach 100%, extremely surpassing the bounds set by Hardy's original test [40] and approaching the framework of GHZ theorem [35] and all-versus-nothing proof [33,34].

Additionally, analogous properties have been extensively studied in two-dimensional systems. In the $(k,2)$ scenario, the maximal violation of Bell inequalities consistently occurs with maximally entangled state; thereby we can obtain the analytical maximum values of Bell expression by substituting $d = 2$ into Eq. (9). Specifically, we have

$$S_{(k,2)}^{\mathrm{max}} = \frac{1}{2} - k\sin^2\left(\frac{\pi}{4k}\right). \quad (11)$$

FIG. 3. Summary of theoretical findings. The subscripts B, d and H, d stand for Bell inequality and Hardy's paradox, respectively, in the d-dimensional system. S_B and S_H represent Bell expression and Hardy's fraction.

Based on the relation between joint probabilities and correlation functions, $P(A_s^i, B_t^j) = \frac{1}{4}\langle[I_2 + (-1)^s A^i] \otimes [I_2 + (-1)^t B^j]\rangle$ (I_2 is the two-dimensional identity matrix), $S_{(k,2)}$ can be reformulated in terms of the generalized CHSH inequality as $S_{(k,2)} = [S_{\mathrm{CHSH}(k)} - 2(k-1)]/4$. As a result, $S_{(k,2)}^{\max}$ relates to Tsirelson's bound of generalized CHSH inequality [41], i.e., $S_{\mathrm{CHSH}(k)}^{\max} = 2k\cos(\pi/2k)$. Combining with the no-signaling bound of CHSH inequality [42], we find that the no-signaling bound of $S_{(2,2)}$ is 0.5, which matches the maximum successful probability of Hardy's nonlocality under the no-signaling principle [43]. Besides, $S_{(2,2)}^{\max} = (\sqrt{2}-1)/2$ (also related to $S_{\mathrm{CHSH}(2)} = 2\sqrt{2}$) corresponds to the information causality bound [44] for both the Bell inequality [45] and Hardy's paradox [46]. Therefore, within our formulation of the CGLMP inequality and the general Hardy's paradox, the link between these two nonlocality arguments becomes clear upon considering the following key facts. (1) The general Hardy's paradox represents a special case of the Bell inequality, with all correlations violating Hardy's paradox also violating Bell inequality. (2) In the limit of large k, these two nonlocality arguments become nearly equivalent, sharing a common bound that matches the no-signaling bound. (3) There is compelling evidence that the bounds for these two nonlocality arguments are nearly identical under certain fundamental principles. Figure 3 summarizes the theoretical findings in the paper.

To elucidate the link between the CGLMP inequality and the general Hardy's paradox, we further compare our experimental result with the Clauser-Horne inequality of Hardy's paradox as discussed in our previous work. Building upon the experimental observations outlined in Ref. [26], we investigate a (k, d) scenario in two specific cases: (1) $k = 2, 3, 4, 5$, and $d = 3$, as depicted in Fig. 2(b), and (2) $k = 2$, and $d = 2, 3, 4, 5, 6$, as illustrated in Fig. 4. It becomes evident that both theoretical and experimental findings underscore the notion that the maximum violation of the CGLMP inequality imposes constraints on the upper limit of Hardy's fraction.

IV. CONCLUSIONS

To summarize, we have presented an experiment to demonstrate CGLMP inequality for multisetting and
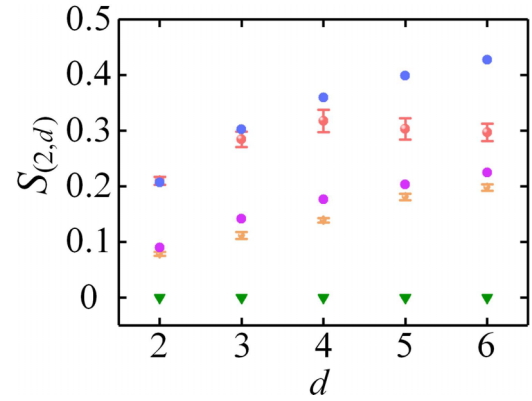

FIG. 4. Comparison of Bell expression and the Clauser-Horne inequality of the general Hardy's paradox in $(2, d)$ scenario. The experimental Bell expression (red plot) compares the theoretically predicted violations (blue plot) by approximate entangled states and the LHV limit (green triangle) with the experiments. The purple plot is the theoretical prediction for the Clauser-Horne inequality of the general Hardy's paradox, while the orange plot bars are experimental results.

multidimensional systems by exploiting two-photon entangled OAM states. The experimental results in the (k, d) scenario with k ranges from 2 to 5 and d ranges from 2 to 6 revealed a remarkable increase in the maximum violation of the CGLMP inequality with higher dimensions and settings. Moreover, our comprehensive theoretical and experimental analysis provides the logical connection between the CGLMP inequality and the general Hardy's paradox. The intriguing results emerge that, even within high-dimensional systems, Hardy's paradox can be considered as a specific instance of the CGLMP inequality. Consequently, both the no-signaling bound and the information causality bound between these two nonlocal structures are found to be equivalent. Besides, in the limit of large k and d, the CGLMP inequality, as well as the general Hardy's paradox, approaches the framework of "all-versus-nothing" proof. Identifying connections between nonlocal theorems is valuable, as it deepens our understanding of nonlocal quantum correlations and unifies their boundaries under some fundamental principles. Furthermore, it enables the reconstruction of suitable nonlocal logical frameworks in practical applications. For instance, one can construct a stronger Hardy-type paradox based on the CH inequality to enhance the probability of nonlocal events [47]. Our findings not only advance the foundational understanding of quantum nonlocality but also hold practical implications for high-dimensional quantum systems. They open up new avenues for further exploration and utilization of quantum nonlocality, particularly in device-independent quantum information tasks, such as quantum key distribution [48–50] and random number generation [51,52], promising enhanced security and efficiency in quantum technologies and protocols.

TABLE I. Comparison of violation between optimal states and approximate state in three dimensions.

Entangled states	$S_{(2,3)}$	$S_{(3,3)}$	$S_{(4,3)}$	$S_{(5,3)}$
$\left\|\psi_{(k,3)}^{\text{opt}}\right\rangle$	0.3050	0.4290	0.4911	0.5279
$\left\|\psi_{3}^{\text{app}}\right\rangle$	0.3021	0.4279	0.4909	0.5274

APPENDIX A: COMPARISON OF VIOLATIONS OF CGLMP INEQUALITIES BETWEEN OPTIMAL STATES AND APPROXIMATE STATES IN THE (k, d) SCENARIO

For each d-dimensional OAM subspace, we experimentally prepare an approximate state $|\psi_d^{\text{app}}\rangle$, which yields a good approximation of the optimal violation of the CGLMP inequality in (k, d) scenarios with $k = 2, 3, 4, 5$. In the following, we use diagonal matrices, $H_{(k,d)}^{\text{opt}} = \text{diag}(\lambda_0, \lambda_1, \ldots, \lambda_{d-1})$ to represent optimal states, $|\psi_{(k,d)}^{\text{opt}}\rangle$, calculated by numeric strategy from Eq. (7). Then, we list the optimal states $|\psi_{(k,d)}^{\text{opt}}\rangle$ and maximum values of Bell expression $S_{(k,d)}$ between optimal states $|\psi_{(k,d)}^{\text{opt}}\rangle$ and approximate states $|\psi_d^{\text{app}}\rangle$ in (k, d) scenarios with k range from 2 to 5 and d range from 2 to 6. In two-dimensional systems, the optimal states are always maximally entangled states, as shown in Eq. (8a). In three-dimensional systems, the optimal states are

$$H_{(2,3)}^{\text{opt}} = \text{diag}(0.6169, 0.4888, 0.6169), \quad (\text{A1a})$$

$$H_{(3,3)}^{\text{opt}} = \text{diag}(0.6070, 0.5129, 0.6070), \quad (\text{A1b})$$

$$H_{(4,3)}^{\text{opt}} = \text{diag}(0.6015, 0.5257, 0.6015), \quad (\text{A1c})$$

$$H_{(5,3)}^{\text{opt}} = \text{diag}(0.5974, 0.5351, 0.5973). \quad (\text{A1d})$$

The comparison of violations of CGLMP inequalities between optimal states and approximate state are very close ($S_{(k,d)}^{\text{opt}} - S_{(k,d)}^{\text{app}} < 0.01$), as shown in Table I. In four-dimensional systems, the optimal states are

$$H_{(2,4)}^{\text{opt}} = \text{diag}(0.5686, 0.4204, 0.4204, 0.5686), \quad (\text{A2a})$$

$$H_{(3,4)}^{\text{opt}} = \text{diag}(0.5521, 0.4418, 0.4418, 0.5521), \quad (\text{A2b})$$

$$H_{(4,4)}^{\text{opt}} = \text{diag}(0.5416, 0.4546, 0.4546, 0.5416), \quad (\text{A2c})$$

$$H_{(5,4)}^{\text{opt}} = \text{diag}(0.5345, 0.4630, 0.4630, 0.5345). \quad (\text{A2d})$$

TABLE II. Comparison of violation between optimal states and approximate state in four dimensions.

Entangled states	$S_{(2,4)}$	$S_{(3,4)}$	$S_{(4,4)}$	$S_{(5,4)}$
$\left\|\psi_{(k,4)}^{\text{opt}}\right\rangle$	0.3648	0.5048	0.5722	0.6111
$\left\|\psi_{4}^{\text{app}}\right\rangle$	0.3591	0.5028	0.5720	0.6102

TABLE III. Comparison of violation between optimal states and approximate state in five dimensions.

Entangled states	$S_{(2,5)}$	$S_{(3,5)}$	$S_{(4,5)}$	$S_{(5,5)}$
$\left\|\psi_{(k,5)}^{\text{opt}}\right\rangle$	0.4063	0.5556	0.6254	0.6649
$\left\|\psi_{5}^{\text{app}}\right\rangle$	0.3987	0.5519	0.6216	0.6572

The comparison of violations of CGLMP inequalities between optimal states and approximate state are very close ($S_{(k,d)}^{\text{opt}} - S_{(k,d)}^{\text{app}} < 0.01$), as shown in Table II. In five-dimensional systems, the optimal states are

$$H_{(2,5)}^{\text{opt}} = \text{diag}(0.5368, 0.3860, 0.3546, 0.3860, 0.5368), \quad (\text{A3a})$$

$$H_{(3,5)}^{\text{opt}} = \text{diag}(0.5151, 0.4033, 0.3795, 0.4033, 0.5151), \quad (\text{A3b})$$

$$H_{(4,5)}^{\text{opt}} = \text{diag}(0.5012, 0.4136, 0.3943, 0.4136, 0.5012), \quad (\text{A3c})$$

$$H_{(5,5)}^{\text{opt}} = \text{diag}(0.4918, 0.4201, 0.4042, 0.4201, 0.4918). \quad (\text{A3d})$$

The comparison of violations of CGLMP inequalities between optimal states and approximate state are very close ($S_{(k,d)}^{\text{opt}} - S_{(k,d)}^{\text{app}} < 0.01$), as shown in Table III. In six-dimensional systems, the optimal states are

$$H_{(2,6)}^{\text{opt}} = \text{diag}(0.5137, 0.3644, 0.3214, 0.3214, 0.3644, 0.5137), \quad (\text{A4a})$$

$$H_{(3,6)}^{\text{opt}} = \text{diag}(0.4878, 0.3780, 0.3452, 0.3452, 0.3780, 0.4878), \quad (\text{A4b})$$

$$H_{(4,6)}^{\text{opt}} = \text{diag}(0.4714, 0.3856, 0.3594, 0.3594, 0.3856, 0.4714), \quad (\text{A4c})$$

$$H_{(5,6)}^{\text{opt}} = \text{diag}(0.4603, 0.3903, 0.3685, 0.3685, 0.3903, 0.4603). \quad (\text{A4d})$$

The comparison of violations of CGLMP inequalities between optimal states and approximate state are very close ($S_{(k,d)}^{\text{opt}} - S_{(k,d)}^{\text{app}} < 0.01$), as shown in Table IV.

APPENDIX B: DETAILED MEASUREMENTS RESULT OF BELL EXPRESSION

In this Appendix, we provide an exhaustive presentation of the measurement outcomes depicted in Fig. 2 across various dimensions of OAM subspaces. Specifically, Fig. 5 illustrates the results obtained for the two-dimensional OAM subspace

TABLE IV. Comparison of violation between optimal states and approximate state in six dimensions.

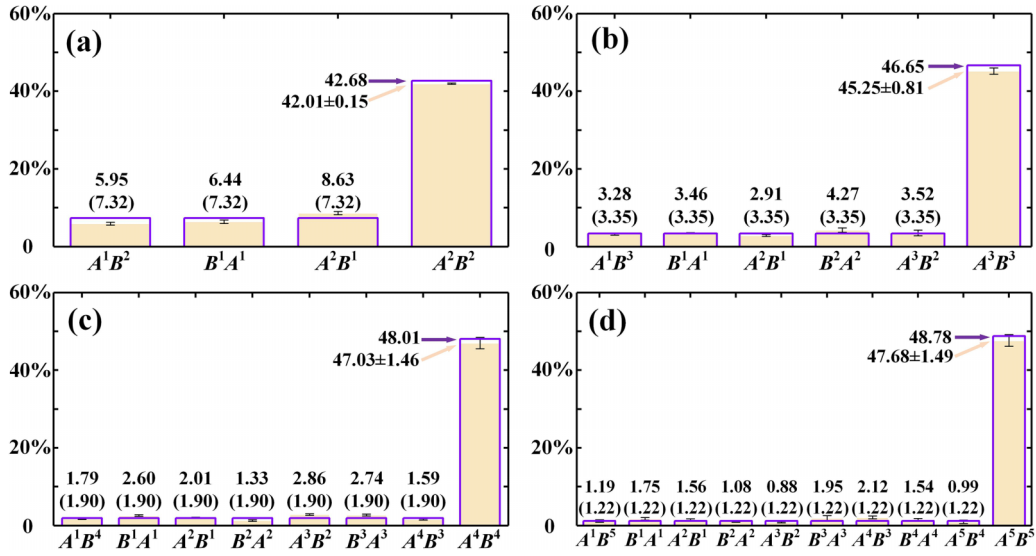| Entangled states	$S_{(2,6)}$	$S_{(3,6)}$	$S_{(4,6)}$	$S_{(5,6)}$
$\left\|\psi_{(k,6)}^{\text{opt}}\right\rangle$	0.4374	0.5927	0.6637	0.7030
$\left\|\psi_{6}^{\text{app}}\right\rangle$	0.4274	0.5894	0.6621	0.6988

FIG. 5. Probabilities of CGLMP inequality in multisetting two-dimensional OAM subspaces with settings (a) $k = 2$, (b) $k = 3$, (c) $k = 4$, and (d) $k = 5$. The empty bars (purple edges) are the theoretical values, while the solid bars (light yellow) are the experimental results. $A^i B^j$ and $B^j A^i$ stand for $P(A^i < B^j)$ and $P(B^j < A^i)$, respectively.

[Fig. 2(a)], while Fig. 6 showcases the corresponding findings for the three-dimensional OAM subspace [Fig. 2(b)]. Furthermore, Figs. 7, 8, and 9 depict the measurement results for the four-dimensional [Fig. 2(c)], five-dimensional [Fig. 2(d)], and six-dimensional [Fig. 2(e)] OAM subspaces, respectively. It is noteworthy that all presented results exhibit a reasonable agreement with quantum-mechanical predictions.

APPENDIX C: BELL EXPRESSION FOR THE MAXIMALLY ENTANGLED STATES $|\psi^{\max}\rangle$

According to Ref. [4], the probability $P(A_s^i, B_t^j)$ can be calculated by taking measurements (4) and (5) into $|\psi_d^{\max}\rangle$ as

$$P\left(A_s^i, B_t^j\right) = \frac{1}{d^3} \frac{\sin^2[\pi(s - t + \alpha_i - \beta_j)]}{\sin^2[\pi(s - t + \alpha_i - \beta_j)/d]}. \quad (C1)$$
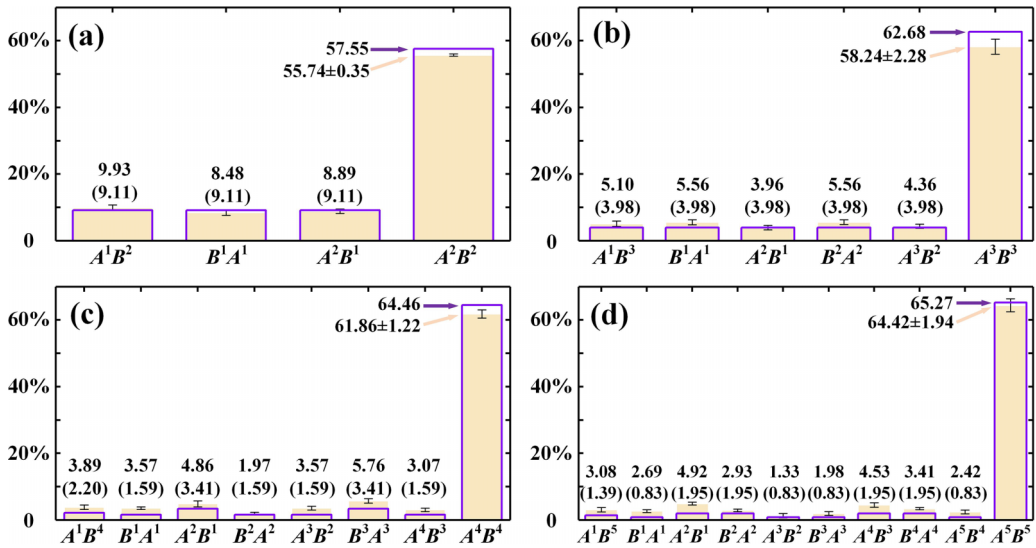

FIG. 6. Probabilities of CGLMP inequality in multisetting three-dimensional OAM subspaces with settings (a) $k = 2$, (b) $k = 3$, (c) $k = 4$, and (d) $k = 5$. The empty bars (purple edges) are the theoretical values, while the solid bars (light yellow) are the experimental results. $A^i B^j$ and $B^j A^i$ stand for $P(A^i < B^j)$ and $P(B^j < A^i)$, respectively.
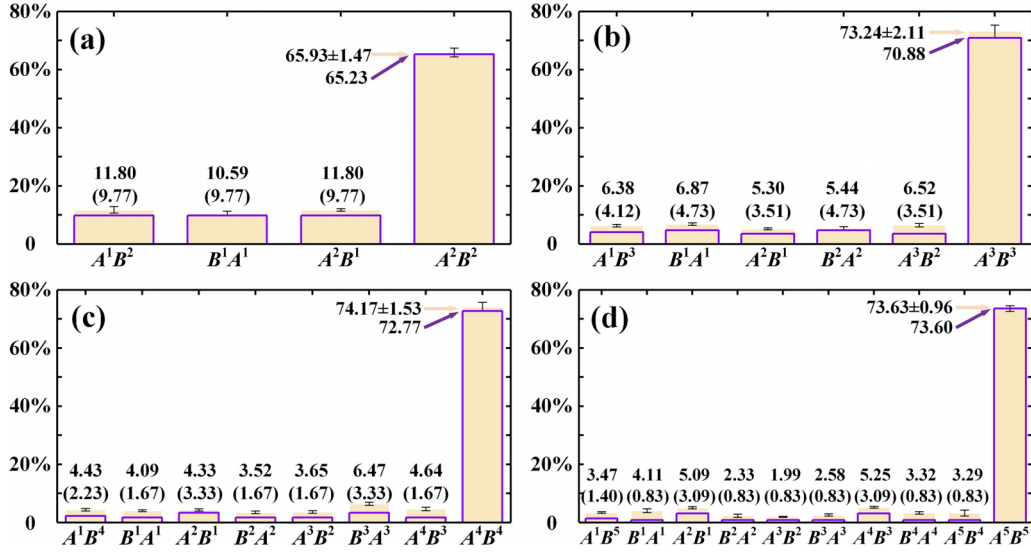
FIG. 7. Probabilities of CGLMP inequality in multisetting four-dimensional OAM subspaces with settings (a) $k = 2$, (b) $k = 3$, (c) $k = 4$, and (d) $k = 5$. The empty bars (purple edges) are the theoretical values, while the solid bars (light yellow) are the experimental results. $A^i B^j$ and $B^j A^i$ stand for $P(A^i < B^j)$ and $P(B^j < A^i)$, respectively.

By combining with $P(A^i < B^j) = \sum_{s=0}^{d-2} \sum_{t=s+1}^{d-1} P(A_s^i, B_t^j)$, we find that, in all the terms of $P(A^i < B^j)$, the situation $s - t = -m$ will occur $d - m$ times; then the probability $P(A^i < B^j)$ can be calculated as

$$P(A^i < B^j) = \sum_{m=1}^{d-1} \frac{1}{d^3} \frac{(d-m)\sin^2[\pi(\alpha_i - \beta_j)]}{\sin^2[\pi(-m+\alpha_i - \beta_j)/d]}. \quad (C2)$$

Besides, we choose the optimal parameters: $\alpha_i = i/k - 1/2k$ for $i = 1, 2, \ldots, k$, and $\beta_j = j/k$ for $i = 1, 2, \ldots, k$, and $\beta_k = 0$.

As each term in Eq. (2) satisfies $\alpha - \beta = \pm 1/2k$, except for $\alpha_k - \beta_k = 1 - 1/2k$, we can calculate Bell expression in terms of (C2) as

$$S_{(k,d)}^{\psi^{\max}} = \frac{1}{d^3} \sum_{m=1}^{d-1} \frac{(d-m)\sin^2\left(\frac{\pi}{2k}\right)}{\sin^2\left[\pi\left(-m+1-\frac{1}{2k}\right)/d\right]}$$
$$- \frac{(2k-1)}{d^3} \sum_{m=1}^{d-1} \frac{(d-m)\sin^2\left(\frac{\pi}{2k}\right)}{\sin^2\left[\pi\left(-m+\frac{1}{2k}\right)/d\right]}. \quad (C3)$$
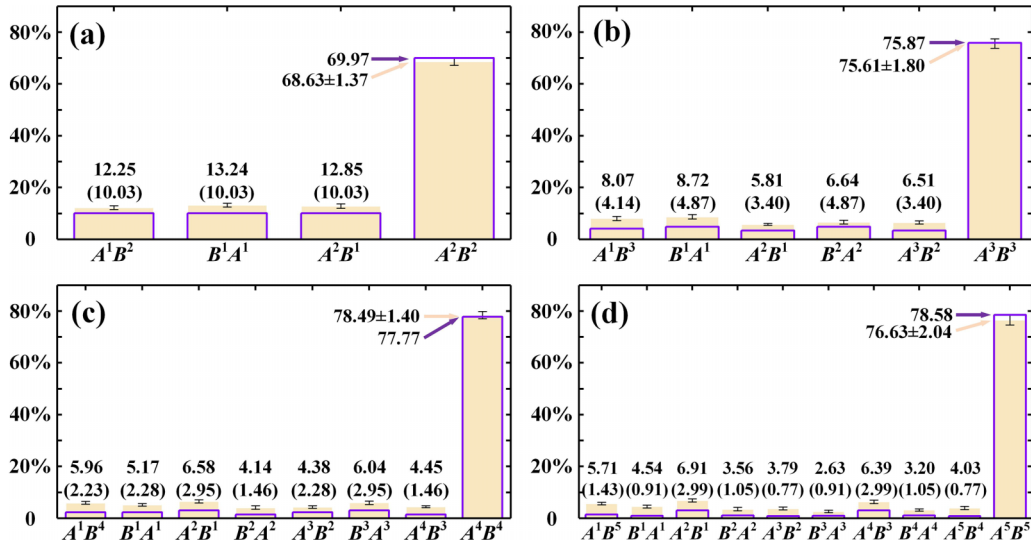

FIG. 8. Probabilities of CGLMP inequality in multisetting five-dimensional OAM subspaces with settings (a) $k = 2$, (b) $k = 3$, (c) $k = 4$, and (d) $k = 5$. The empty bars (purple edges) are the theoretical values, while the solid bars (light yellow) are the experimental results. $A^i B^j$ and $B^j A^i$ stand for $P(A^i < B^j)$ and $P(B^j < A^i)$, respectively.
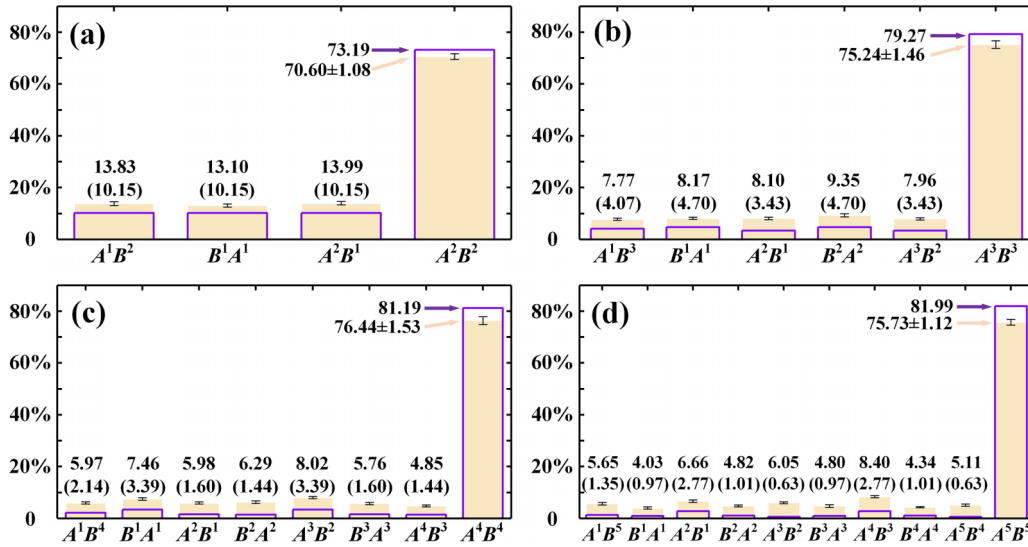
FIG. 9. Probabilities of CGLMP inequality in multisetting six-dimensional OAM subspaces with settings (a) $k = 2$, (b) $k = 3$, (c) $k = 4$, and (d) $k = 5$. The empty bars (purple edges) are the theoretical values, while the solid bars (light yellow) are the experimental results. $A^i B^j$ and $B^j A^i$ stand for $P(A^i < B^j)$ and $P(B^j < A^i)$, respectively.

[1] A. Einstein, B. Podolsky, and N. Rosen, Can quantum-mechanical description of physical reality be considered complete? Phys. Rev. **47**, 777 (1935).

[2] J. S. Bell, On the Einstein-Podolsky-Rosen paradox, Phys. Phys. Fiz. **1**, 195 (1964).

[3] N. Brunner, D. Cavalcanti, S. Pironio, V. Scarani, and S. Wehner, Bell nonlocality, Rev. Mod. Phys. **86**, 419 (2014).

[4] D. Collins, N. Gisin, N. Linden, S. Massar, and S. Popescu, Bell inequalities for arbitrarily high-dimensional systems, Phys. Rev. Lett. **88**, 040404 (2002).

[5] A. C. Dada, J. Leach, G. S. Buller, M. J. Padgett, and E. Andersson, Experimental high-dimensional two-photon entanglement and violations of generalized Bell inequalities, Nat. Phys. **7**, 677 (2011).

[6] S. Zohren and R. D. Gill, Maximal violation of the Collins-Gisin-Linden-Massar-Popescu inequality for infinite dimensional states, Phys. Rev. Lett. **100**, 120406 (2008).

[7] A. Tavakoli, S. Zohren, and M. Pawłowski, Maximal non-classicality in multi-setting Bell inequalities, J. Phys. A: Math. Theor. **49**, 145301 (2016).

[8] A. Salavrakos, R. Augusiak, J. Tura, P. Wittek, A. Acín, and S. Pironio, Bell inequalities tailored to maximally entangled states, Phys. Rev. Lett. **119**, 040402 (2017).

[9] J. Barrett, A. Kent, and S. Pironio, Maximally nonlocal and monogamous quantum correlations, Phys. Rev. Lett. **97**, 170409 (2006).

[10] R. Colbeck and R. Renner, Hidden variable models for quantum theory cannot have any local part, Phys. Rev. Lett. **101**, 050403 (2008).

[11] Y. Fu, W. Liu, X. Ye, Y. Wang, C. Zhang, C.-K. Duan, X. Rong, and J. Du, Experimental investigation of quantum correlations in a two-qutrit spin system, Phys. Rev. Lett. **129**, 100501 (2022).

[12] X.-M. Hu, C. Zhang, B.-H. Liu, Y. Guo, W.-B. Xing, C.-X. Huang, Y.-F. Huang, C.-F. Li, and G.-C. Guo, High-dimensional Bell test without detection loophole, Phys. Rev. Lett. **129**, 060402 (2022).

[13] N. Miklin, A. Chaturvedi, M. Bourennane, M. Pawlowski, and A. Cabello, Exponentially decreasing critical detection efficiency for any Bell inequality, Phys. Rev. Lett. **129**, 230403 (2022).

[14] N. T. Islam, C. C. W. Lim, C. Cahall, J. Kim, and D. J. Gauthier, Provably secure and high-rate quantum key distribution with time-bin qudits, Sci. Adv. **3**, e1701491 (2017).

[15] Y. Ding, D. Bacco, K. Dalgaard, X. Cai, X. Zhou, K. Rottwitt, and L. K. Oxenlwe, High-dimensional quantum key distribution based on multicore fiber using silicon photonic integrated circuits, npj Quantum Inf. **3**, 25 (2017).

[16] M. Huber and M. Pawłowski, Weak randomness in device-independent quantum key distribution and the advantage of using high-dimensional entanglement, Phys. Rev. A **88**, 032309 (2013).

[17] X.-M. Hu, W.-B. Xing, B.-H. Liu, D.-Y. He, H. Cao, Y. Guo, C. Zhang, H. Zhang, Y.-F. Huang, C.-F. Li, and G.-C. Guo, Efficient distribution of high-dimensional entanglement through 11 km fiber, Optica **7**, 738 (2020).

[18] J. Barrett, L. Hardy, and A. Kent, No signaling and quantum key distribution, Phys. Rev. Lett. **95**, 010503 (2005).

[19] H. Lu, Z. Hu, M. S. Alshaykh, A. J. Moore, Y. Wang, P. Imany, A. M. Weiner, and S. Kais, Quantum phase estimation with time-frequency qudits in a single photon, Adv. Quantum Technol. **3**, 1900074 (2020).

[20] D. González-Cuadra, T. V. Zache, J. Carrasco, B. Kraus, and P. Zoller, Hardware efficient quantum simulation of non-Abelian gauge theories with qudits on Rydberg platforms, Phys. Rev. Lett. **129**, 160501 (2022).

[21] S. Omanakuttan, A. Mitra, E. J. Meier, M. J. Martin, and I. H. Deutsch, Qudit entanglers using quantum optimal control, PRX Quantum **4**, 040333 (2023).

[22] W. Sun and Z. Wei, Equivalence checking of quantum circuits by nonlocality, npj Quantum Inf. **8**, 139 (2017).

[23] S. McArdle, S. Endo, A. Aspuru-Guzik, S. C. Benjamin, and X. Yuan, Quantum computational chemistry, Rev. Mod. Phys. **92**, 015003 (2020).

[24] Y. Chi, J. Huang, Z. Zhang, Z. Zhang, J. Mao, Z. Zhou, X. Chen, C. Zhai, J. Bao, T. Dai, H. Yuan *et al.*, A programmable qudit-based quantum processor, Nat. Commun. **13**, 1166 (2022).

[25] L. Lu, L. Xia, Z. Chen, L. Chen, T. Yu, T. Tao, W. Ma, Y. Pan, X. Cai, Y. Lu, S. Zhu, and X.-S. Ma, Three dimensional entanglement on a silicon chip, npj Quantum Inf. **6**, 30 (2020).

[26] D. Zhang, X. Qiu, T. Ma, W. Zhang, and L. Chen, Orbitalangular-momentum-based experimental test of Hardy's paradox for multisetting and multidimensional systems, Phys. Rev. A **101**, 053821 (2020).

[27] M. J. Padgett, Orbital angular momentum 25 years on [Invited], Opt. Express **25**, 11265 (2017).

[28] A. Forbes, M. de Oliveira, and M. R. Dennis, Structured light, Nat. Photon. **15**, 253 (2021).

[29] L.-J. Kong, Y. Sun, F. Zhang, J. Zhang, and X. Zhang, High-dimensional entanglement-enabled holography, Phys. Rev. Lett. **130**, 053602 (2023).

[30] M. Erhard, M. Krenn, and A. Zeilinger, Advances in high dimensional quantum entanglement, Nat. Rev. Phys. **2**, 365 (2020).

[31] A. Mair, A. Vaziri, G. Weihs, and A. Zeilinger, Entanglement of the orbital angular momentum states of photons, Nature (London) **412**, 313 (2001).

[32] S. Kunkri, S. K. Choudhary, A. Ahanj, and P. Joag, Nonlocality without inequality for almost all two-qubit entangled states based on Cabello's nonlocality argument, Phys. Rev. A **73**, 022346 (2006).

[33] Z.-B. Chen, J.-W. Pan, Y.-D. Zhang, Č. Brukner, and A. Zeilinger, All-versus-nothing violation of local realism for two entangled photons, Phys. Rev. Lett. **90**, 160408 (2003).

[34] T. Yang, Q. Zhang, J. Zhang, J. Yin, Z. Zhao, M. Żukowski, Z.-B. Chen, and J.-W. Pan, All-versus-nothing violation of local realism by two-photon, four-dimensional entanglement, Phys. Rev. Lett. **95**, 240406 (2005).

[35] D. M. Greenberger, M. A. Horne, A. Shimony, and A. Zeilinger, Bells theorem without inequalities, Am. J. Phys. **58**, 1131 (1990).

[36] L. Mancinska and S. Wehner, A unified view on Hardy's paradox and the Clauser-Horne-Shimony-Holt inequality, J. Phys. A: Math. Theor. **47**, 424027 (2014).

[37] H. X. Meng, J. Zhou, Z. P. Xu, H. Y. Su, T. Gao, F. L. Yan, and J. L. Chen, Hardy's paradox for multisetting high-dimensional systems, Phys. Rev. A **98**, 062103 (2018).

[38] S. Ecker, F. Bouchard, L. Bulla, F. Brandt, O. Kohout, F. Steinlechner, R. Fickler, M. Malik, Y. Guryanova, R. Ursin, and M. Huber, Overcoming noise in entanglement distribution, Phys. Rev. X **9**, 041042 (2019).

[39] S. S. Bhattacharya, A. Roy, A. Mukherjee, and R. Rahaman, All-versus-nothing violation of local realism from the Hardy paradox under no-signaling, Phys. Rev. A **92**, 012111 (2015).

[40] R. Rabelo, Y. Z. Law, and V. Scarani, Device-independent bounds for Hardy's experiment, Phys. Rev. Lett. **109**, 180401 (2012).

[41] S. Wehner, Tsirelson bounds for generalized Clauser-Horne-Shimony-Holt inequalities, Phys. Rev. A **73**, 022110 (2006).

[42] A. Acín and L. Masanes, Certified randomness in quantum physics, Nature (London) **540**, 213 (2016).

[43] J. L. Cereceda, Quantum mechanical probabilities and general probabilistic constraints for Einstein-Podolsky-Rosen-Bohm experiments, Found. Phys. Lett. **13**, 427 (2000).

[44] M. Pawłowski, T. Paterek, D. Kaszlikowski, V. Scarani, A. Winter, and M. Zukowski, Information causality as a physical principle, Nature (London) **461**, 1101 (2009).

[45] J. L. Cereceda, Chained Clauser-Horne-Shimony-Holt inequality for Hardy's Ladder test of nonlocality, Quantum Inf. Process. **15**, 1779 (2016).

[46] A. Ahanj, S. Kunkri, A. Rai, R. Rahaman, and P. S. Joag, Bound on Hardy's nonlocality from the principle of information causality, Phys. Rev. A **81**, 032103 (2010).

[47] M. Yang, H. X. Meng, J. Zhou, Z. P. Xu, Y. Xiao, K. Sun, J. L. Chen, J. S. Xu, C. F. Li, and G. C. Guo, Stronger Hardy-type paradox based on the Bell inequality and its experimental test, Phys. Rev. A **99**, 032103 (2019).

[48] W. Zhang, T. van Leent, K. Redeker, R. Garthoff, R. Schwonnek, F. Fertig, S. Eppelt, W. Rosenfeld, V. Scarani, C. C.-W. Lim, and H. Weinfurter, A device independent quantum key distribution system for distant users, Nature (London) **607**, 687 (2022).

[49] W.-Z. Liu, Y.-Z. Zhang, Y.-Z. Zhen, M.-H. Li, Y. Liu, J. Fan, F. Xu, Q. Zhang, and J.-W. Pan, Toward a photonic demonstration of device-independent quantum key distribution, Phys. Rev. Lett. **129**, 050502 (2022).

[50] F. Xu, Y.-Z. Zhang, Q. Zhang, and J.-W. Pan, Device independent quantum key distribution with random postselection, Phys. Rev. Lett. **128**, 110506 (2022).

[51] S. Pironio, A. Acín, S. Massar, A. Boyer de la Giroday, D. N. Matsukevich, P. Maunz, S. Olmschenk, D. Hayes, L. Luo, T. A. Manning, and C. Monroe, Random numbers certified by Bell's theorem, Nature (London) **464**, 1021 (2010).

[52] C. R. i. Carceller, K. Flatt, H. Lee, J. Bae, and J. B. Brask, Quantum vs noncontextual semi-device-independent randomness certification, Phys. Rev. Lett. **129**, 050501 (2022).